The Journal of Experimental Biology 215, 3096-3105

doi:10.1242/jeb.071704

RESEARCH ARTICLE

The neural mechanisms of antennal positioning in flying moths

Anand Krishnan*, Sunil Prabhakar*, Subashini Sudarsan* and Sanjay P. Sane†

National Centre for Biological Sciences, Tata Institute of Fundamental Research, GKVK Campus, Bangalore 560065, India

*These authors contributed equally to this work
†Author for correspondence (sane@ncbs.res.in)

SUMMARY

In diverse insects, the forward positioning of the antenna is often among the first behavioral indicators of the onset of flight. This behavior may be important for the proper acquisition of the mechanosensory and olfactory inputs by the antennae during flight. Here, we describe the neural mechanisms of antennal positioning in hawk moths from behavioral, neuroanatomical and neurophysiological perspectives. The behavioral experiments indicated that a set of sensory bristles called Böhm's bristles (or hair plates) mediate antennal positioning during flight. When these sensory structures were ablated from the basal segments of their antennae, moths were unable to bring their antennae into flight position, causing frequent collisions with the flapping wing. Fluorescent dye-fills of the underlying sensory and motor neurons revealed that the axonal arbors of the mechanosensory bristle neurons spatially overlapped with the dendritic arbors of the antennal motor neurons. Moreover, the latency between the activation of antennal muscles following stimulation of sensory bristles was also very short (<10 ms), indicating that the sensorimotor connections may be direct. Together, these data show that Böhm's bristles control antennal positioning in moths *via* a reflex mechanism. Because the sensory structures and motor organization are conserved across most Neoptera, the mechanisms underlying antennal positioning, as described here, are likely to be conserved in these diverse insects.

Supplementary material available online at http://jeb.biologists.org/cgi/content/full/215/17/3096/DC1

Key words: antennal position, Böhm's bristles, insect flight.

Received 27 February 2012; Accepted 3 May 2012

INTRODUCTION

Insect antennae are multimodal sensory structures that provide olfactory, mechanosensory, hygrosensory and thermosensory information to the insect nervous system (Schneider, 1964). These sensory inputs guide insect flight in several ways. On the shorter (approximately single wing stroke) time scales, antennal mechanosensory feedback is thought to be of key importance for flight control in both non-Dipteran (e.g. Gewecke et al., 1974; Sane et al., 2007; Sane et al., 2010) and Dipteran (Gewecke and Schlegel, 1970; Mamiya et al., 2011) insects, whereas on the longer (of the order of multiple wing strokes) time scales feedback from other modalities such as vision and olfaction also influences their overall flight trajectories (Kennedy and Marsh, 1974; Willis and Arbas, 1991; Willis and Arbas, 1998; Verspui and Gray, 2009; Vickers, 2000). The central processing of mechanosensory and olfactory inputs is clearly separated within the insect deutocerebrum. Whereas the olfactory input is primarily processed by interneurons within the antennal lobe, the majority of the antennal mechanosensory neurons located in the basal segments of the antennae project in an area of the deutocerebrum called the antennal motor and mechanosensory center (AMMC) (Homberg et al., 1989), although some wind-sensory receptors have recently been reported to also arborize in the antennal lobe (Han et al., 2005).

Among insects of diverse Neopteran orders including Lepidoptera, Hymenoptera, Coleoptera and many non-brachyceran Diptera, the forward positioning of the antenna is one of the first behaviors signaling the onset of flight. Because antennal mechanosensory and olfactory feedback actively influence flight trajectories, the proper placement of antennae relative to the body may be a behavior of crucial importance for the optimal acquisition of these inputs. During flight, these insects maintain the position of the antenna in a definite relationship with respect to their air speeds (Heran, 1957; Gewecke, 1974). In the fruit fly *Drosophila melanogaster*, the antennae are both passively and actively positioned in a direction opposite to the visual motion (Mamiya et al., 2011). Similar behaviors have also been observed during walking [stick insects (Dürr et al., 2001); cockroaches (Okada and Toh, 2006)] and other activities such as feeding [e.g. ants (Ehmer and Gronenberg, 1997)] in other Neoptera. The active control of antennal position requires that insects be able to sense the position of their own antennae. In the cockroach *Periplaneta americana*, scapal hair plates encode the instantaneous position of the antenna and provide the brain with information about the objects encountered by the antenna, thus playing a central role in enabling the use of the antenna as a tactile organ (Okada and Toh, 2000; Okada and Toh, 2001). In contrast, Sphingid moths typically tuck their antennae under the wings when resting. When the moths are ready to fly, they rotate their antennae forward and keep them specifically positioned for flight (Dorsett, 1962). In the absence of this behavior, their wings and antennae would collide, thereby impeding both wing motion and antennal function (supplementary material Fig. S1).

What is the nature of sensorimotor integration underlying the antennal positioning behavior? Here, we address this question using multiple approaches. First, we show that antennal positioning behavior during flight in the Oleander hawk moth *Daphnis nerii* is primarily mediated by the mechanosensory Böhm's bristles (Böhm,

1911) located on the basal segments of their antennae. The neurons underlying the Böhm's bristles are stimulated by the movement of bristles in and out of the inter-joint folds during gross antennal movements (Fig. 1A,B; supplementary material Movie 1). As previously described in the tobacco hornworm moth, *Manduca sexta* (Kloppenburg et al., 1997), the antennal movements in *Daphnis nerii* are also accomplished by two sets of antennal muscles: a set of five extrinsic muscles that move the scape relative to the head capsule, and a set of four intrinsic muscles that move the pedicel relative to the scape. Böhm's bristles are arranged in two and three discrete fields on the pedicel and scape, respectively. Using dye-filling techniques and confocal imaging, we investigated the sensorimotor circuitry of the Böhm's bristle mechanosensors as well as the motor neurons that control activity in the antennal muscles. Finally, we used neurophysiological techniques to stimulate the bristles while recording from the antennal muscles. Together, these data provide insight into the basic neural mechanisms of antennal positioning in flying moths.

MATERIALS AND METHODS

Moth breeding

All experiments reported here were conducted on the adults of laboratory-bred Oleander hawk moths, *D. nerii* (Linnaeus 1758). The larvae of these moths were reared on the leaves of two types of host plants *Nerium oleander* and *Tabernaemontana divaricata* placed within mesh-topped boxes to enable easy ventilation. Pupae were embedded in sawdust and transferred to wire-mesh cages. Post-emergence, the adult moths were exposed to a natural day–night cycle. For breeding, we maintained about 4–8 moths at a 1:1 sex ratio within a 1 m^3 Plexiglas chamber with their host plants. After 2–3 days, we collected the eggs from the host plants and placed them under conditions of ambient temperature and humidity until hatching and during larval stages. Under these conditions, egg-to-egg life cycle of the moth was approximately 45 days.

Scanning electron microscopy

To obtain fine resolution images of the Böhm's bristles, we used scanning electron microscopy on antennae excised from freshly killed hawk moths (Fig. 1A,B). The antennae samples were dehydrated through a series of 10%, 20%, 30%, 50%, 75%, 90% and 100% alcohol and then placed on carbon tapes on aluminium stubs. We placed the stubs in an ultrasonicator for 1 min to remove particulate matter and a desiccator for 30 s to remove residual moisture. The sample was then sputter-coated with gold for ~30 s and the samples were imaged using scanning electron microscopy (EVO LS10).

Tethering procedure

All behavioral experiments were conducted on tethered 1–2 day old adult *D. nerii* moths. To cold-anesthetize the moths, we placed them at –20°C until they became inactive. The anesthetized moths were then ventrally tethered to an aluminium post (2 mm diameter, 5–6 cm length) at the sternum using a mixture of cyanoacrylate adhesive and sodium bicarbonate (see Sane and Jacobson, 2006). This procedure ensured that moths remained tethered for the entire duration of the experiments.

Measurement of antennal positioning behavior

Ablation of mechanosensors

All experimental procedures involving ablation of Böhm's bristles were carried out on the right antenna, whereas the left antenna was left unimpaired and served as an internal control. In bristle-ablated and sham-treated moths, we first reduced the activity of the moths by placing them on ice, and ablated their Böhm's bristles using a 30 gauge hypodermic needle.

The experimental insects were divided into six groups. In the first group (control), the bristles were left untouched but moths underwent cold-anesthesia similar to experimental insects. Control moths were allowed to recover after tethering without any further procedures. In the second group (sham), we brushed a needle over the bristles without breaking them but otherwise handled the moth similar to the experimental cases. In the third group (scapal and pedicellar bristles ablated), we ablated both the scapal and the pedicellar Böhm's bristles. In the fourth group (scapal bristles ablated), only the scapal bristles were ablated whereas the pedicellar bristles were left intact. In the fifth group (pedicellar bristles ablated), the pedicellar bristles were ablated but not the scapal bristles. Finally, in the sixth group (restricted pedicel–flagellum joint), we used cyanoacrylate adhesive to glue the pedicel–flagellar joint. This treatment eliminated or substantially reduced the input to the Johnston's organs, which span the pedicel–flagellar joint and are stimulated by mechanical distortions of this joint (Sane et al., 2007).

At end of each experiment, the moths were placed at –20°C. We closely examined them post-mortem using light microscopy to ensure that experimental manipulations were clean and restricted to those intended for the experiment.

Electromagnetic perturbation of the insect antennae

To perturb the antennal position at a distance during tethered flight, we attached a small piece of iron (<10% of the antennal mass) to the right antenna of the tethered moth and used an electromagnet (36 V, 2 A DC power supply) placed beyond the antennal length to move the antenna from its set position (Fig. 1C). A custom-designed LabVIEW protocol (National Instruments, Austin, TX, USA) delivered pulse trains (pulse width 300 ms at 700 ms intervals; in some earlier experiments the pulse width was 1 s with an interval of 1 s) to the electromagnet *via* an AD converter (National Instruments, USB 6229). A red LED connected in parallel with the electromagnet indicated when the electromagnet was on in our video recordings. We recorded between 8 and 10 pulses or perturbations for each moth. For digitization, we selected only those trials where the stimulus onset resulted in a clearly detectable (>5 deg; range 5–20 deg) movement of the antenna (Fig. 1F, inset). Because it was not always possible to precisely position the electromagnet relative to the antenna of the live moth, the maximum perturbed angle of the antennal position varied from trial to trial. To compare the kinematics of recovery, we therefore normalized each inter-antennal angle trace relative to its peak value.

Acquisition, digitization and analysis of high-speed video

After each treatment, we allowed the tethered moths to recover for 2 h and filmed their flight using two synchronized Phantom v7.3 high-speed cameras (Vision Research, Wayne, NJ, USA) at 1000 frames s^{-1} (100 µs exposure time). This frame rate ensured about 30–33 frames per wing beat, thus providing a sufficiently detailed temporal resolution of antennal movement. One camera was positioned above the moth to provide a dorsal perspective and another camera was frontally positioned. Two black spots marked on the antenna ~0.5 cm from their tip eased the digitization. Flight was elicited using tactile stimuli or by gently blowing air on the animal. We calibrated the fixed cameras before and after each experiment. A custom-written Matlab code (Mathworks, Natick, MA, USA) for calibration and digitization (Hedrick, 2008) was used

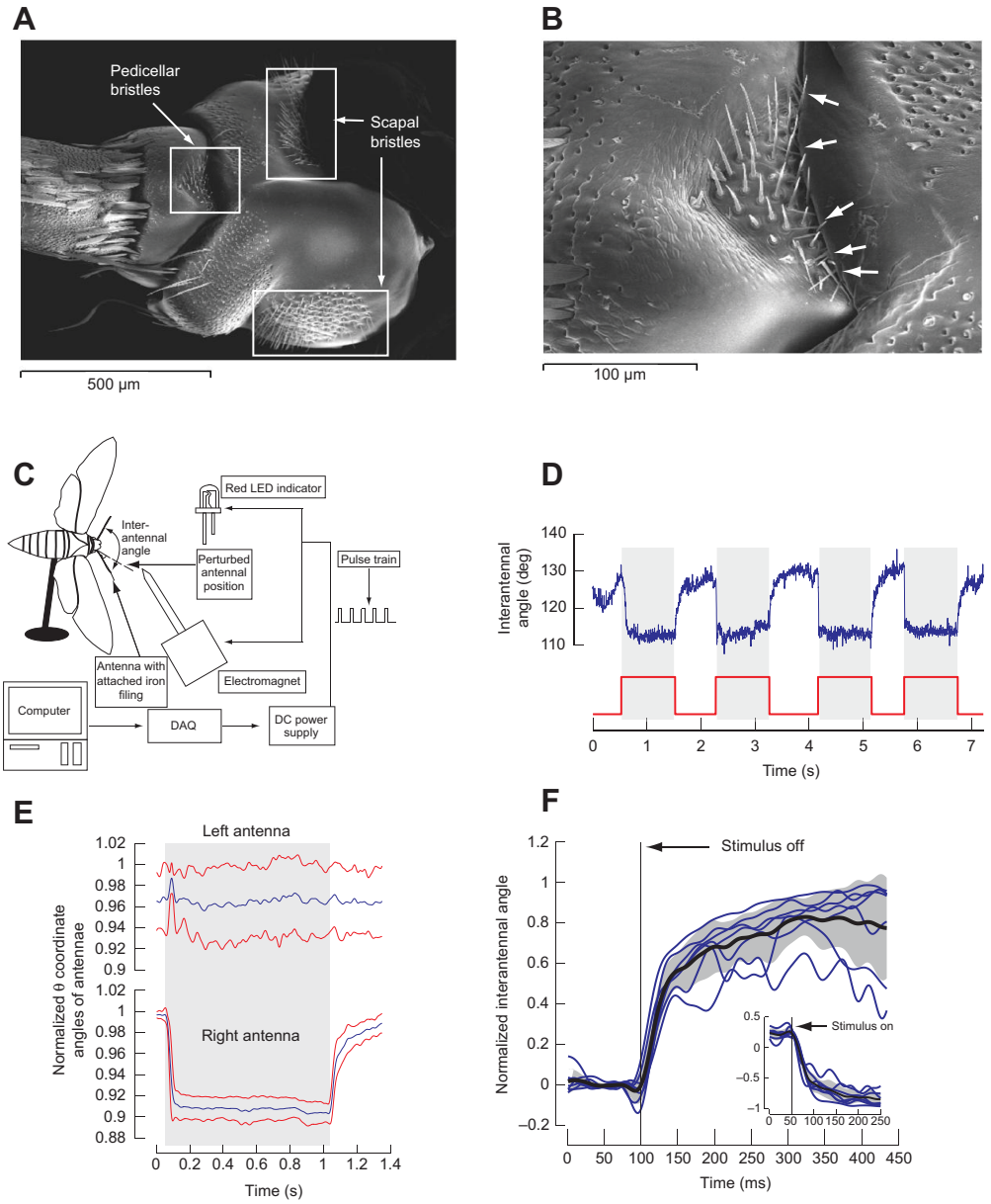

Fig. 1. (A) Scanning electron micrograph of the base of the antenna showing the scapal and pedicellar Böhm's bristles. (B) Close-up of a pedicellar bristle field, showing some bristles deflected by the cuticular rim of the scape (white arrows; see also supplementary material Movie 1), as would occur during antennal movements. (C) Schematic diagram of the experiment to study antennal positioning by perturbing the antenna with an electromagnet. (D) A representative raw trace showing recovery of the inter-antennal angle to its original value (blue trace) following successive perturbations with the electromagnet. The red trace represents the state of the electromagnet (on/off) as measured using a red LED. (E) Representative normalized theta (azimuthal) angle coordinates of the unperturbed left antenna (top) and the perturbed right antenna (bottom) showing ipsilaterality of antennal positioning. Each blue trace is a mean of seven trials from the same moth, while the red lines represent standard deviations. Each trace was normalized to its own peak. The gray shaded areas in D and E represent the duration when the stimulus is on. (F) Clipped stimulus offsets across the datasets show stereotypy in the recovery of antennal position. The blue traces represent a mean plot for each individual moth (N=7) while the group mean is shown in black with the gray shaded area representing 1 s.d. The inset shows the perturbation delivered to the antennae at stimulus onset.

to convert the Cartesian coordinates of the antennae into spherical coordinates to calculate the inter-antennal angles (Sane et al., 2007). Digitization error was estimated by measuring the constancy of the antennal length as a function of time across a sample of digitized videos. Error estimates were between 0.5% and 3.2%, within acceptable limits of measurement error.

The antennal positions for each treatment were plotted as rose diagrams of frequency distributions of inter-antennal angles (measured from 200–300 frames of video digitized per moth) across experimental treatments using Oriana (Kovach Computing Services, Anglesey, UK) (Fig. 2). The data showed significant directionality of the mean vector (length of mean vector >0.9 in all cases), and fit to a Von Mises distribution with significant non-uniformity (P<0.01 using both the Rayleigh test and Rao's spacing test for circular uniformity) (Batschelet, 1981). Hence, we used the parametric Watson–Williams F-test (multisample, pairwise) to compare circular means of the interantennal angle across datasets (Zar, 1999).

Neuroanatomy of the Böhm's bristles

To visualize the neural circuitry that underlies the antennal mechanosensory and motor system, we cold-anesthetized the moths, inserted them into a sawn-off syringe tube and immobilized their head and thorax using molten dental wax. The exposed dorsal head capsule was then descaled and dissected to gain access to the intrinsic and extrinsic antennal muscles for fluorescent dye-fills. The organization of the antennal muscles in *D. nerii* is identical to that of *M. sexta* (Kloppenburg et al., 1997). Because sensory neurons are more likely to stimulate muscles from the same segment, we filled either the intrinsic musculus scapo–pedicellaris posterior [Ms-pp (Niehaus and Gewecke, 1978)] muscles in combination with a sensory fill of the posterior pedicellar bristles (pPB), or the extrinsic musculus tentorio–scapalis lateralis [Mt-sl (Niehaus and Gewecke, 1978) or anterior depressor muscle (ADM) (Kloppenburg et al., 1997)] in combination with the medial scapal bristles (mSB). For the purpose of this paper, these muscle–bristle pairs may be seen as representative combinations for both dye-fills and

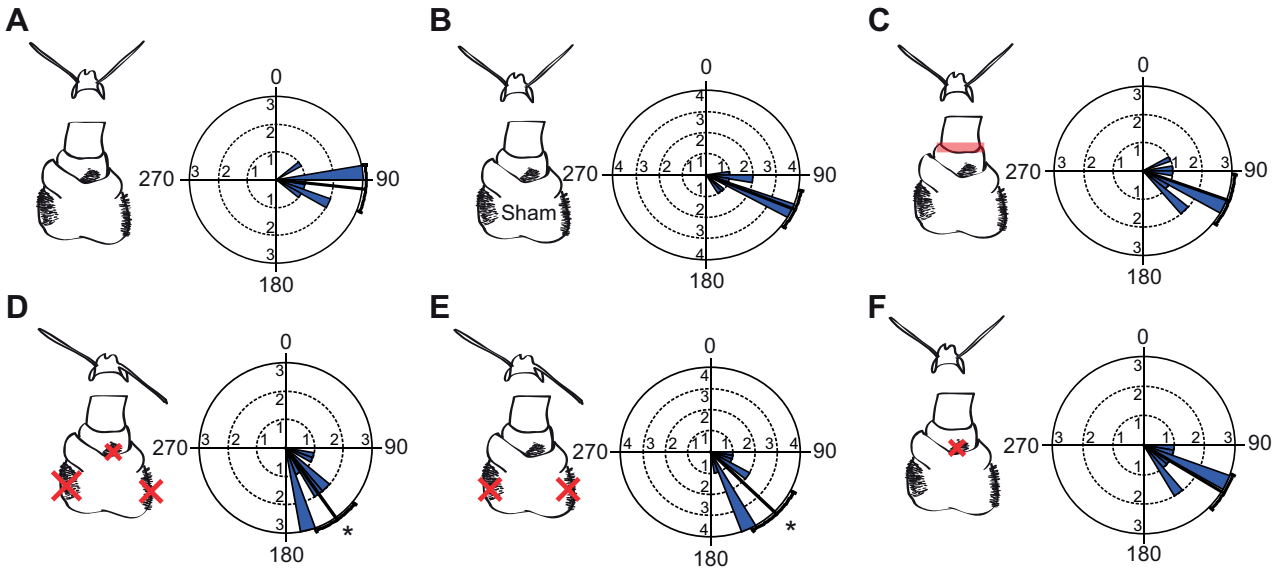

Fig. 2. Rose diagrams (bin size 10 deg) representing inter-antennal angles of tethered flying hawk moths. All manipulations were performed on the right antenna only. (A) Intact control moths with unmanipulated antennae (N=9). (B) Sham-treated moths show no significant (P>0.05) increase in inter-antennal angle (N=10). (C) Reducing input to the Johnston's organs by restricting the pedicellar–flagellar joint does not significantly alter antennal positioning (N=9). (D) Ablation of all fields of Böhm's bristles on the right antenna causes improper antennal positioning, as represented by a significant (*P<0.01) increase in inter-antennal angles. The unmanipulated left antenna assumes normal position (N=10). (E) Ablation of only scapal bristle fields resulted in a significant increase in inter-antennal angle (*P<0.05), similar to moths with all bristles ablated (N=10). (F) Ablation of only pedicellar bristle fields had no effect on inter-antennal angles (N=9). The black line represents the circular mean angle of each dataset, with 95% confidence intervals represented by the black arc. Each concentric circle represents increasing frequency in steps of 1.

electrophysiology. More detailed neuroanatomy of other combinations will be published elsewhere.

We used aqueous Texas Red dextran (3000 MW, emission peak 615 nm; Molecular Probes, Invitrogen, Carlsbad, CA, USA) for backfills of antennal muscles and aqueous fluorescein–dextran (3000 MW, emission peak 521 nm; Molecular Probes) to fill sensory neurons exposed post-ablation of the Böhm's bristles. The animals were kept alive for at least 24 h after dye filling to enable full permeation of the dye, following which the brain was fixed in 4% paraformaldehyde for 8–10 h and dissected out. The dissected brains were dehydrated through an alcohol series (50–100% ethanol), cleared with xylene and whole-mounted in DPX. Slides were imaged with a laser-scanning confocal microscope (Olympus FV1000) at 10×/20× magnification (Fig. 3). We collected 1 µm optical sections of the brain using sequential scanning with a 543 nm He–Ne laser and a 488 nm Kr–Ar laser to detect red and green fluorescence, respectively. Images thus obtained were processed with ImageJ (National Institutes of Health, Bethesda, MD, USA).

In some cases, we cryo-sectioned the brain to obtain a clearer view of the sensorimotor double fills (Fig. 3C,F). After filling and dissecting as described above, we incubated the brain in a 30% solution of sucrose in phosphate-buffered saline (PBS) for 24–48 h at 4°C and embedded and froze it in Jung Tissue Freezing Medium. The tissue embedded in this section block was sliced into 60 µm sections using a Leica CM 1850 cryostat at temperatures below –20°C. Sections were mounted in VectaShield H-1000 (Vector Laboratories, Burlingame, CA, USA) and imaged using a confocal microscope (40×/60×, oil immersion).

Electromyography of the antennal muscles

To record the activity of antennal muscles in response to stimulation of the Böhm's bristles, we first immobilized adult moths by placing them in a sawn-off syringe tube as described above. The preparation was mounted on a pneumatic table under a swiveling dissection microscope (after 1 h of recovery), and the left antenna (in which we performed all recordings) was inserted into a glass capillary and glued in place at approximately the 5th annulus of the flagellum. We restricted the pedicel–flagellar joint using cyanoacrylate glue to ensure that only the scape was free to move. Antennal muscles were exposed using a similar procedure to motor neuron backfills, and a grounding electrode was inserted into the frontal area of the head cuticle.

We recorded responses of the extrinsic muscles (Mt-sl) to stimulation of the scapal bristles (mSB), and intrinsic muscles (Ms-pp) to stimulation of pedicellar bristles (pPB) using a tungsten recording electrode (5 µm diameter, 2 MΩ impedance; FHC, Bowdoin, ME, USA) mounted on an extracellular head stage (Dagan 8024, Minneapolis, MN, USA). We mechanically stimulated the bristles with a brush mounted on the shaft of a stepper motor. The motion of the brush was tracked using an optical sensor. Using this apparatus, we delivered short 50 ms impulse stimuli (40–60 trials/moth) to the Böhm's bristles using pCLAMP10.0 *via* an AD converter (DigiData 1322A; Axon Instruments, Union City, CA, USA) while keeping the antenna immobile. The impulse response of the system provided measures of response latency. We also delivered blank stimuli where the brush moved in air without contacting any surfaces to identify potential sources of electrical noise due to brush movement. Muscle responses were amplified using a dual intracellular amplifier (Dagan IX2 700) and line frequency noise was eliminated using a HumBug noise eliminator (Quest Scientific, North Vancouver, BC, Canada). After each recording, we backfilled the muscles at the recording sites with Texas Red dextran and the stimulated bristle fields with fluorescein dextran. After keeping the moth alive for 24 h, we fixed, dissected and imaged the brain using confocal microscopy.

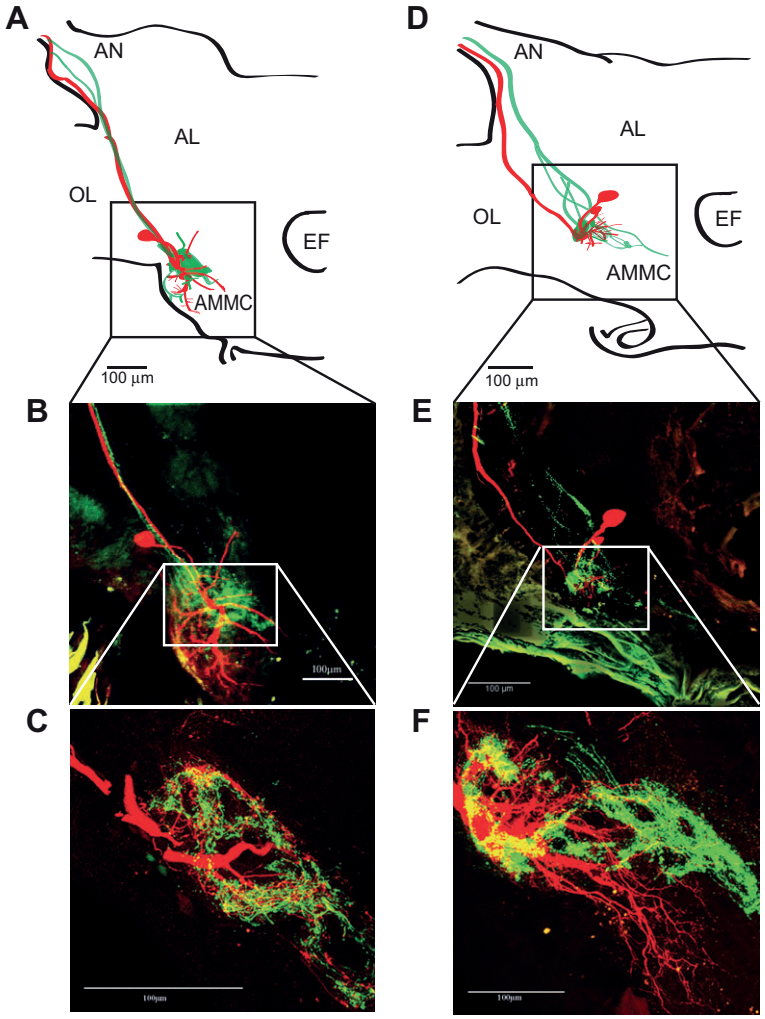

Fig. 3. The sensory arbors of the Böhm's bristles (green: fluorescein–dextran) overlap with the dendritic branches of antennal muscle motor neurons (red: Texas Red–dextran). (A–C) The sensory arbors of the pPB pedicellar bristles (see Materials and methods for description of anatomy) overlap with the dendrites of the Ms-pp intrinsic antennal motor neurons in the antennal motor and mechanosensory center (AMMC). (D–F) The axonal arbors of mSB scapal bristle neurons overlap with the dendrites of Mt-sl extrinsic antennal muscle (two shown here) within the AMMC. (A,D) Traces of the confocal images of the filled neurons (green, sensory; red, motor). AN, antennal nerve; AL, antennal lobe; EF, esophageal foramen; OL, optic lobe. (B,E). Confocal images of the arborizations in the AMMC (scale bar, 100 μm). (C,F) A 60 μm thick section of the AMMC showing heavy overlap between sensory and motor arbors (scale bar, 100 μm).

Analysis of the electromyogram recordings of antennal muscles

The raw electromyogram (EMG) data were filtered through a band-pass filter with a low cut-off at 20 Hz and a high cut-off at 700 Hz. We used a threshold-based spike sorting program (pCLAMP10.0) to identify spikes, and constructed a matrix of spike times (represented as a raster plot in Fig. 4C). Spike data across trials for each experiment were pooled into 1 ms bins (although we used 5 ms bins to plot Fig. 4C) and the binned data were used to construct histograms of the firing rates across trials. To account for the differences in basal and peak responses between records, the histograms were normalized with respect to the peak firing rate. We calculated the average firing rate as the mean of all data points across the first 3 s of the instantaneous firing rate change plot, including the stimulus phase.

To determine the latency of firing after a stimulus, we used two criteria. First, we determined the 'latency to significant shift in firing' as the point at which the firing rate crossed 5 s.d. from the mean mentioned above. Second, we calculated the 'latency to peak firing rate' as the point at which the firing rate reached its peak value of 1. Stimulus traces were imported into Matlab, passed through a 45 Hz low-pass filter, time aligned and stored in a matrix, which was then used to calculate the averaged stimulus trace. We estimated the start point of the stimulus as the time at which the sensor voltage changed by 1% of its peak value. This start point was used as a reference point to calculate latencies of the muscle response.

RESULTS

Antennal positioning is a robust, ipsilaterally confined behavior

To quantify antennal positioning behavior, we first reconstituted it in tethered flying *D. nerii* by attaching a small iron filing to the tip of each antenna, and delivering pulsed electromagnetic perturbations to displace the antennae from their normal flight position. Under these conditions, the antenna rapidly recovered its original position when the stimulus was released. The perturbation of one antenna did not affect the contralateral antenna, indicating that antennal positioning behavior is ipsilaterally confined (Fig. 1E). Moreover, the recovery was biphasic with a fast phase lasting 80–100 ms after the release of the antenna, followed by a slower correction of position lasting 250–300 ms (Fig. 1F).

Ablation of Böhm's bristles affects antennal positioning

To examine the role of Böhm's bristles in antennal positioning, we compared the inter-antennal angles of the bristles-intact control group with those of moths that were sham-treated or had scapal and/or pedicellar bristles ablated, or whose pedicel–flagellar joint was restricted to reduce input to the Johnston's organ (Fig. 2). The mean inter-antennal angle of the control group was 96.17±20.02 deg (N=9; Fig. 2A). These moths positioned their antennae symmetrically, always bringing forward their antennae prior to flight initiation. This behavior was not significantly different in the sham-

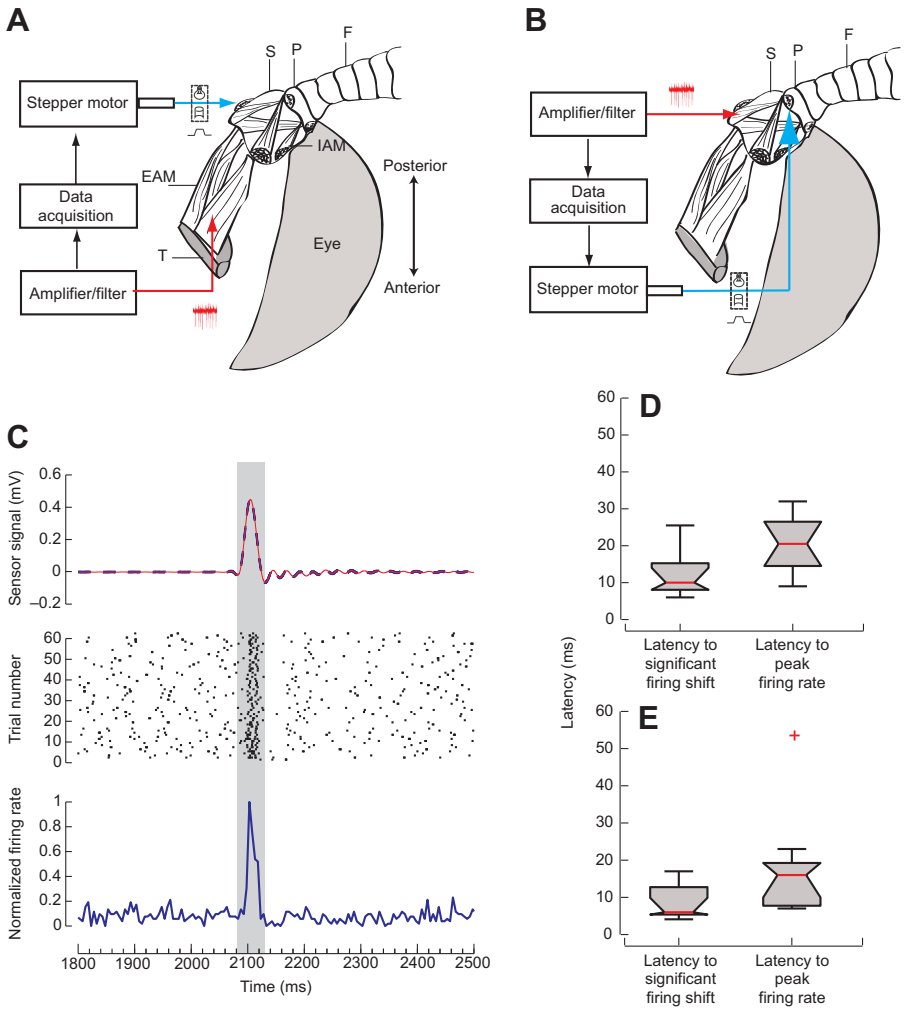

Fig. 4. (A,B) Schematic diagram of electromyogram recordings from antennal muscles (red) while stimulating Böhm's bristles (blue). (A) Recording from the Mt-sl extrinsic muscle while stimulating the mSB scapal bristles. (B) Recording from the Ms-pp intrinsic muscle while stimulating the pPB pedicellar bristles (S, scape; P, pedicel; F, flagellum; EAM, extrinsic antennal muscle; IAM, intrinsic antennal muscle; T, tentorium). (C) Representative data (60 trials) from a single moth showing mean stimulus waveform (top) as red trace with standard deviations represented in blue, spiking raster plots of the response to stimulation (middle) and the normalized peri-stimulus time histogram (5 ms bins) (bottom). (D,E) Distribution of latencies to significant firing shift (5 s.d. from the mean) and to peak firing rate of extrinsic muscles (Mt-sl) with scapal bristle (mSB) stimulation (N=8) (D) and intrinsic muscles (Ms-pp) with pedicellar bristle (pPB) stimulation (N=9) (E). The red plus sign indicates a statistical outlier.

treated group in which the mean inter-antennal angle was 113.45±17.91 deg (N=10; Fig. 2B), ruling out the possibility that experimental handling of the antennae caused any changes in antennal positioning response. Similarly, restricting the pedicel–flagellar junction with cyanoacrylate glue did not significantly alter this behavior (circular mean 110.02±22.39 deg; N=9; Fig. 2C), indicating that the mechanosensory input from the Johnston's organs (which is severely reduced when the pedicel–flagellum junction is glued) is not involved in the antennal positioning response.

In contrast to the above treatments, ablation of the scapal and pedicellar Böhm's bristles significantly altered the antennal positioning response. When both the scapal and pedicellar bristles on the right antenna were ablated, the moths failed to move their antenna forward during flight, instead keeping them in their resting position and thus causing repeated collisions with the wing during flapping (Fig. 2D; also see supplementary material Fig. S1). In these moths, the antennae were capable of spontaneous movement, suggesting that the observed effect was not due to muscle damage, but to an inability to actively maintain the antenna in its normal flight position. We measured inter-antennal angles of 144.67±20.95 deg (N=10; Fig. 2D), significantly greater than control (P<0.001) and sham (P<0.01) groups. In contrast to the bristle-ablated right antennae, the untreated left antennae showed normal positioning, again suggesting that the antennal positioning behavior had no contralateral influence (supplementary material Movie 1).

Ablation of only the scapal Böhm's bristles (circular mean 135.26±24.61 deg; N=10; Fig. 2E) also caused the inter-antennal angles to be significantly different from the control (P<0.01; Fig. 2A) and sham-treated (P<0.05; Fig. 2B) groups. However, the ablation of only pedicellar bristles had no visible effect on gross positioning of the antenna, and the measured inter-antennal angles (circular mean 121.52±15.95 deg; N=9; Fig. 2F) differed significantly from those of the control group (P<0.05) but not the sham group. Variability of the inter-antennal angles was comparable across experimental treatments.

From these experiments, we can conclude that the gross antennal positioning response is primarily driven by input from the scapal Böhm's bristles, and not the Johnston's organs or the pedicellar bristles. We could not, however, rule out a subtler role in fine tuning the set-point of antennal position, especially for pedicellar bristles.

Axonal arbors of bristle sensory neurons spatially overlap with dendrites of antennal motor neurons

To visualize the neural circuitry underlying the Böhm's bristles and the antennal muscles, we filled the sensory neurons (medial scapal bristles and posterior pedicellar bristles) and the motor neurons innervating the representative extrinsic (Mt-sl) and intrinsic (Ms-pp) muscles with fluorescent dyes in two different emission ranges. The sensory neurons were marked by aqueous fluorescein dextran (3000 MW) and the motor neurons by Texas Red dextran (3000 MW).

Confocal imaging of both the dye-filled medial scapal (mSB) and posterior pedicellar (pPB) bristles neurons revealed that their axons passed *via* the antennal nerve and arborized ipsilaterally in the region of the deutocerebrum called the AMMC (Rospars, 1988) (Fig. 3A,D). None of the observed bristle fills had contralateral projections, in agreement with our behavioral observation that antennal positioning behavior was ipsilaterally confined. We recovered one to two motor neurons with similar morphology from each muscle backfill. The dendritic arbors of these motor neurons were located in the AMMC, while their cell bodies were located dorsally or dorsolaterally with respect to the arbor (Kloppenburg et al., 1997). Ascending axonal tracts of the motor neurons were in close juxtaposition with the descending sensory tracts within the antennal nerve. We observed extensive spatial overlap of these dendritic arbors with the axonal arbors of the sensory neurons innervating the bristles (Fig. 3; see also supplementary material Movie 2) similar to that reported in bees (Kloppenburg, 1995).

To obtain a more magnified view of the extent of the overlap of sensory axonal and motor dendritic arbors, we cryo-sectioned the dissected brain preparations of dye-filled moths into 60 µm sections, and imaged them at 40×/60× magnification under oil immersion. This allowed us to substantially improve the signal-to-noise ratio of the confocal imaging. Even at these magnifications, we observed extensive spatial overlap of the red (motor) and green (sensory) dyes, indicating the possibility of monosynaptic connectivity between the bristle mechanosensory and antennal motor neurons.

Antennal muscles respond to stimulation of Böhm's bristles

The spatial overlap between sensory axonal and motor dendritic arbors provides only indirect evidence for the presence of a monosynaptic reflex arc. To examine whether these two neurons connect with each other *via* functional synapses that enable information flow from one neuron to another, we mechanically stimulated specific Böhm's bristle fields with a moving brush and recorded EMGs from the antennal muscles (Fig. 4A,B).

We conducted two sets of experiments to measure the latency between sensory stimulation and antennal muscle activation. First, we stimulated the medial scapal bristles (mSB) while recording from the extrinsic Mt-sl muscle (Fig. 4A). Second, we stimulated the posterior pedicellar bristles (pPB) while recording from the intrinsic Ms-pp muscle (Fig. 4B). The background activity in both these sets of muscles varied from low to high levels of spontaneous firing. The mechanical stimulation consisted of short (50 ms) stimuli to the bristles, which were tracked using voltage traces on an optical motion sensor (Fig. 4C, top panel). In the majority of the cases, the muscles responded to the impulse stimulus with a sharply stimulus-locked excitatory response, which returned to background levels after the stimulus had ceased (Fig. 4C, middle panel), although in very rare cases we also observed inhibitory responses (data not shown). These data were then pooled into 1 ms bins and normalized to plot the average firing rate as a function of time (Fig. 4C, bottom panel, although this uses a 5 ms bin size for plotting purposes only). We used two measures of antennomotor response latency. For the first, we calculated the value of the 'latency to significant firing shift' defined as the time duration between the stimulus onset and the time instant when the firing rate crossed 5 s.d. from the mean. The second and more conservative measure was the 'latency to peak firing rate'. Post-recording, we filled the muscles by applying fluorescent dextran dyes at the site of recording. This procedure allowed us to recover antennal motor neurons in ~60% of recordings.

The extrinsic Mt-sl muscle showed a significant shift in firing within 12.2±6.4 ms (median 10 ms) of the stimulus start point (N=8). Peak firing was achieved in 20.5±7.8 ms (median 20.5 ms) (Fig. 4D). The Ms-pp intrinsic muscle recording also showed a significant shift in firing rate in 8.4±4.6 ms (N=9; median 6 ms), with peak firing rate being achieved in 18.2±14.1 ms (median 16 ms; Fig. 4E). The latencies calculated above include the time taken for the brush to contact the bristle fields, which probably caused the variability seen in our latency measurements. Moreover, because these latency values also include the conduction times from the bristle neurons to the AMMC and the AMMC to the muscles, and also the synaptic delays between the sensory and motor neurons as well as at neuromuscular junctions, additional interneurons are unlikely to be part of the sensorimotor circuit. We therefore hypothesize that the antennal positioning behavior described here is likely a monosynaptic reflex arc. Moreover, because the significant shifts in muscle firing occur in less than a third of a wing stroke, while peak firing rates were achieved within the time scale of half a wing stroke (wing beat frequency of *D. nerii* ~33 Hz, data not shown), these reflexes can allow an animal to obtain information about its antennal position within a fraction of its wing stroke.

DISCUSSION

We combined evidence from behavioral, neuroanatomical and neurophysiological experiments to understand the sensorimotor mechanisms of antennal positioning in moths. The behavioral experiments indicated that mechanosensory Böhm's bristles at the base of the antennae mediate the antennal positioning response. Additional evidence from neuroanatomical studies showed that the axonal arbors of the mechanosensory bristle neurons arborize in the AMMC and spatially overlap with dendrites of the antennal motor neurons. The neurophysiological investigation revealed rapid response latencies between sensory stimulation of the Böhm's bristles to activity in the antennal muscles.

Role of antennal positioning in flight

The multimodal sensory feedback from antennae influences flight over short and long time scales. For instance, mechanosensory feedback from the Johnston's organs within the antennae is conducted *via* axons of larger diameters to the brain and is involved in flight control and stabilization on time scales of the order of single wing strokes (Sane et al., 2007). In addition, antennal mechanosensory feedback has also been implicated in air flow sensing over the insect body (Gewecke and Heinzel, 1980; Heinzel and Gewecke, 1987; Gewecke and Niehaus, 1981; Niehaus, 1981). Because antennae of insects belonging to diverse orders (Lepidoptera, Coleoptera, Hymenoptera and certain non-Brachyceran Diptera) are held in a fixed position relative to the head during flight, the antennal positioning behavior is thought to bear some relevance to flight.

In the case of *Drosophila*, lateral antennal positioning precedes a change in wing amplitude of the contralateral wing during turns (Mamiya et al., 2011). In the case of tethered bees (Heran, 1957) and locusts (Gewecke, 1974), the antenna actively swings forward as the insect increases its flight speed. Although a similar behavior was not observed in the butterfly *Aglais urticae* (Gewecke and Niehaus, 1981), the observations in tethered bees and locusts led to suggestions that antennal positioning may be crucial for ensuring that the Johnston's organs are maintained in their operating range (Gewecke and Heinzel, 1980; Heinzel and Gewecke, 1987). One implication of this hypothesis is that sensory feedback from the Johnston's organs directly or indirectly modulates the antennal

positioning response. However, our observation that antennal position in moths with a glued pedicel–flagellar joint (Fig. 2C) was not significantly different from that of control or sham-treated moths (Fig. 2A,B) does not support this hypothesis. Alternatively, because the Johnston's organs situated in the passive pedicel–flagellar junction provide important balance-related cues during flight (Sane et al., 2007), a behavioral switch from movable to constrained antennal positioning reduces the additional ambiguity arising from the changing spatial position of the Johnston's organs. According to this hypothesis, the inputs from Böhm's bristles and Johnston's organs are essentially separate. Whereas the Böhm's bristles and perhaps other sensory modalities such as vision provide feedback about antennal position to the central nervous system, the Johnston's organs independently sense antennal vibrations in the absence of the ambiguities introduced by the gross antennal movements, but provide no feedback to the antennal motor system.

In addition to mechanosensory function, the precise positioning of the antenna may also be important for olfaction during flight. In Lepidoptera and other insects, the periodicity of the inflow of air due to flapping means that insects receive odor in pulses rather than in a continuous fashion (Sane and Jacobson, 2006; Horsmann et al., 1983). Recent work on olfactory sensitivity (Tripathy et al., 2010) showed that the hawk moth, *M. sexta*, can track odor pulses up to 30 Hz with peak sensitivity at wing beat frequencies. During flapping, proper positioning of the antenna may help ensure that the antenna receives these pulses over the maximal length of its receptive surface. Besides flight, precise antennal positioning has also been noted in several behaviors in other insects. For instance, in cockroaches, hair plates (homologous to Böhm's bristles) are involved in proprioception of antennal movements (Okada and Toh, 2000). Similarly, in the trap jaw ant *Odontomachus*, a behavior involving a rapid antennal withdrawal just prior to the snapping of the mandibles ensures that the antennae are protected from the mandible strike (Ehmer and Gronenberg, 1997). Hence, although the study reported here focuses on the role of mechanosensory feedback due to Böhm's bristles in antennal positioning, we cannot rule out the possibility that other inputs such as vision or olfaction also influence the activity of the antennal motor neurons, as has been noted in recent studies in the case of *D. melanogaster* (Mamiya et al., 2011).

The connectivity of the sensory and motor neurons

The structure and organization of the neural circuit proposed here for the antennal positioning reflex bears much resemblance to a few other examples of monosynaptic reflexes previously described in locusts (Burrows, 1975), cockroaches (Pearson et al., 1976) and flies (Fayyazuddin and Dickinson, 1996). In locusts, Burrows showed that mechanosensory input from the wing stretch receptor forms monosynaptic connections with flight motor neurons, with synaptic latency values of about 1 ms from stimulation in the stretch receptor nerve to excitatory responses in the wing depressor motor neurons, and latencies of 4–6 ms to inhibitory response in the wing elevator motor neurons (Burrows, 1975). Like the neural circuit described in this paper, the stretch receptor–flight motor neuronal system was also restricted to the ipsilateral side. Similar monosynaptic connections have also been shown between trochanteral hair plate afferents in the metathoracic leg analogous to the Böhm's bristles, and the femur flexor and extensor motor neurons analogous to the intrinsic and extrinsic antennomotor neurons (Pearson et al., 1976). In the case of flies, monosynaptic reflexes may be found in the connections between the mechanosensory neurons underlying the haltere campaniform sensillae and the b1 motor neurons (mnb1), which innervate the first basalar (b1) steering muscle. In this case, the reflex was found to be mediated by a mixed synapse with a slow polysynaptic (chemical; latency 3.1±0.7 ms) and a fast monsynaptic (electrotonic; synaptic latency 0.87±0.02 ms) component (Fayyazuddin and Dickinson, 1996). Extracellular recordings of the same system reveal latencies between haltere nerve stimulation and b1 muscle activity to be 3–4 ms (Mielke and Heide, 1993). Similarly, Trimarchi and colleagues have shown that the latency values from the mechanical stimulation of hair plate sensors on the prothoracic leg to the extrinsic muscle ('muscle 29'), which remotes and abducts the coxa, is approximately 10.3±0.4 ms, indicative of monosynaptic reflexes between hair plate sensors and extrinsic motor neurons in *D. melanogaster* (Trimarchi et al., 1999).

The behavioral (Figs 1, 2) and neuroanatomical (Fig. 3) data described here show that the antennal mechanosensory–motor reflex is ipsilateral and mediated by the Böhm's bristles located only on that antenna (Fig. 1E). The latency values of significant firing shift in the antennal muscles in response to stimulation of Böhm's bristles are less than 10 ms (median 6 ms for intrinsic muscles, 10 ms for extrinsic muscles) including measurements as low as 5–6 ms in both intrinsic and extrinsic muscles. The latency of the antennal positioning response described here falls well within the range of latencies in the above examples, and hence is also likely to represent

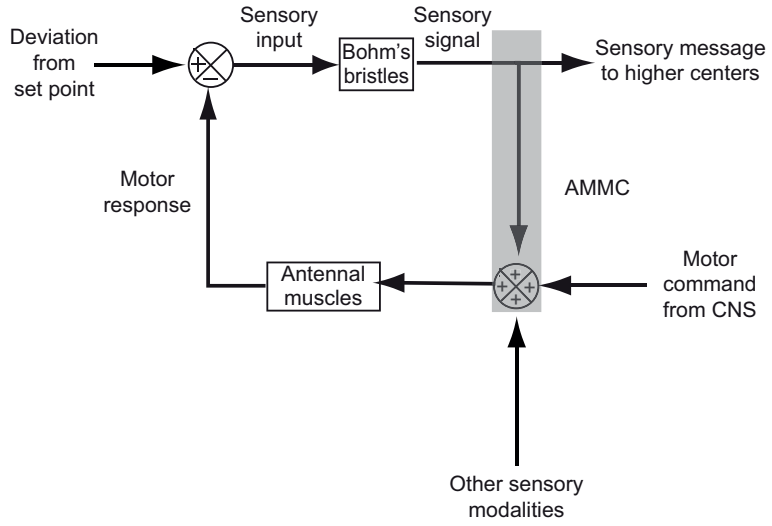

Fig. 5. Schematic model of a putative feedback loop controlling antennal positioning. Inputs from the Böhm's bristles trigger motor commands to the antennal muscles. This restores the antenna to its original position. Inputs from other sensory systems to the AMMC may modulate the functioning of this system.

a similar underlying connectivity. Moreover, because these latency values include the time for the moving brush to contact the bristles, the conduction times from sensory activation to the AMMC and from the AMMC to motor neuronal activation, and the synaptic delays at the neuromuscular junction of the recorded muscle and within the central nervous system, the antennal positioning behavior is most likely mediated *via* monosynaptic connections between the sensory and motor neurons within the AMMC. This is also indicated by the double dye-fill experiments in which the sensory axonal arbors lie in spatial apposition to the motor dendritic arbors. A more rigorous test of this hypothesis requires detailed electrophysiology involving recording of the synaptic potentials within the postsynaptic motor neurons (e.g. Pearson et al., 1976; Burrows, 1975) and neuroanatomical investigations to directly visualize these synapses (e.g. Atwood et al., 1993).

Together, these data suggest that the antennal mechanosensory–motor integration involves a negative feedback loop such that any gross motion of the antenna from a set point position causes stimulation of the mechanosensory Böhm's bristles (supplementary material Movie 1), which in turn activate the antennal motor neurons *via* putative monosynaptic connections. The motor neurons then activate the set of antennal muscles, causing the antenna to return to its set point position, and thus ensure that the antennal position is maintained over the course of flight. A preliminary model that summarizes these hypotheses is shown in Fig. 5. Alternatively, the antennal mechanosensory–motor circuit investigated here may be involved only in bringing the antennae to their initial set-point positions, following which the antennal position is maintained by co-activation of the extensor and flexor extrinsic antennal muscles, which primarily control the gross antennal position.

Generality of the antennal positioning response

Although the actual contexts of antennal positioning in several of the examples discussed above vary from tactile sensation [e.g. cockroaches (Harley et al., 2009; Okada and Toh, 2006), bees (Scheiner et al., 2005)], odor-related antennation (Kisch and Haupt, 2009), protective withdrawal [ants (Ehmer and Gronenberg, 1997)], gravity detection (Markl, 1962), flight (this paper), etc., its mediation and control *via* Böhm's bristles (or hair plates) is likely to be a fairly general phenomenon. Indeed, the presence of Böhm's bristles or hair plate structures is a fairly conserved feature in the antennae of most (but not all) Neopteran insects (H. H. Sant and S.P.S., unpublished observations). Similarly, the antennal muscle and motor neuron organizations in diverse Neopteran insects have also been well described [bees (Kloppenburg, 1995), moths (Kloppenburg et al., 1997), crickets (Honegger et al., 1990), locusts (Bauer and Gewecke, 1991), stick insects (Dürr et al., 2001), cockroaches (Baba and Comer, 2008)] (for a review, see Schneider, 1964). In all these insects, although the exact numbers of muscles differ between orders, they can be subdivided into extrinsic and intrinsic muscles, with motor neurons arborizing in the AMMC. Where they exist, the organization of the Böhm's bristle fields may also substantially vary from one insect order to another. For instance, the Böhm's bristles in Lepidoptera, Blattodea and Orthoptera are organized as discrete fields on the scape and pedicel, whereas in Hymenoptera they are uniformly spread over the entire surface of the scape (Markl, 1962). It remains to be seen whether the spatial organization of these fields is indicative of the degree of antennal motion, or whether the underlying pattern of neuronal arborization and sensorimotor connectivity is indicative of their role during antennal positioning behavior.

ACKNOWLEDGEMENTS

We are grateful to Mr M. Kemparaju for moth breeding, Prof. K. Chandrashekara from GKVK, Bangalore for advice on moth colony, Taruni Roy for Scanning Electron Microscopy, Dr K. S. Krishnan for electrophysiology equipment, Janani Subramanian for help with neuroanatomy and Amit Singh for filming supplementary material Movie 1.

FUNDING

Funding for this study was provided by the Air Force Office of Scientific Research (AFOSR), Asian Office of Aerospace Research and Development (AOARD), International Technology Center-Pacific (ITC-PAC) and Ramanujan Fellowship to S.P.S. from the Department of Science and Technology, Government of India.

REFERENCES

Atwood, H. L., Govind, C. K. and Wu, C. F. (1993). Differential ultrastructure of synaptic terminals on ventral longitudinal abdominal muscles in *Drosophila* larvae. *J. Neurobiol.* **24**, 1008-1024.
Baba, Y. and Comer, C. M. (2008). Antennal motor system of the cockroach, *Periplaneta americana*. *Cell Tissue Res.* **331**, 751-762.
Batschelet, E. (1981). *Circular Statistics in Biology*. London, UK: Academic Press.
Bauer, C. K. and Gewecke, M. (1991). Motoneuronal control of antennal muscles in *Locusta migratoria*. *J. Insect Physiol.* **37**, 551-562.
Böhm, L. K. (1911). Die Antennale Sinnesorgane der Lepidopteren. *Arbeiten aus dem Zoologischen Instituten der Universität Wien und der Zoologischen Station in Triest* **14**, 219-246.
Burrows, M. (1975). Monosynaptic connexions between wing stretch receptors and flight motoneurones of the locust. *J. Exp. Biol.* **62**, 189-219.
Dorsett, D. A. (1962). Preparation for flight by hawk-moths. *J. Exp. Biol.* **39**, 579-588.
Dürr, V., König, Y. and Kittmann, R. (2001). The antennal motor system of the stick insect *Carausius morosus*: anatomy and antennal movement pattern during walking. *J. Comp. Physiol. A* **187**, 131-144.
Ehmer, B. and Gronenberg, W. (1997). Proprioceptors and fast antennal reflexes in the ant *Odontomachus* (Formicidae, Ponerinae). *Cell Tissue Res.* **290**, 153-165.
Fayyazuddin, A. and Dickinson, M. H. (1996). Haltere afferents provide direct, electrotonic input to a steering motor neuron in the blowfly, Calliphora. *J. Neurosci.* **16**, 5225-5232.
Gewecke, M. (1974). The antennae of insects as air-current sense organs and their relationship to the control of flight. In *Experimental Analysis of Insect Behaviour* (ed. L. B. Browne), pp. 100-113. Berlin, Germany: Springer.
Gewecke, M. and Heinzel, H.-G. (1980). Aerodynamic and mechanical properties of the antennae as air-current sense organs inLocusta migratoria. *J. Comp. Physiol. A* **139**, 357-366.
Gewecke, M. and Niehaus, M. (1981). Flight and flight control by the antennae in the small tortoiseshell (*Aglais urticae* L., Lepidoptera). *J. Comp. Physiol.* **145**, 249-256.
Gewecke, M. and Schlegel, P. (1970). Vibrations of antenna and their significance for flight control in blowfly *Calliphora erythrocephala*. *Z. Vgl. Physiol.* **67**, 325-362.
Gewecke, M., Heinzel, H.-G. and Philippen, J. (1974). Role of antennae of dragonfly *Orthetrum cancellatum* in flight control. *Nature* **249**, 584-585.
Han, Q., Hansson, B. S. and Anton, S. (2005). Interactions of mechanical stimuli and sex pheromone information in antennal lobe neurons of a male moth, Spodoptera littoralis. *J. Comp. Physiol. A* **191**, 521-528.
Harley, C. M., English, B. A. and Ritzmann, R. E. (2009). Characterization of obstacle negotiation behaviors in the cockroach, *Blaberus discoidalis*. *J. Exp. Biol.* **212**, 1463-1476.
Hedrick, T. L. (2008). Software techniques for two- and three-dimensional kinematic measurements of biological and biomimetic systems. *Bioinspir. Biomim.* **3**, 034001.
Heinzel, H. G. and Gewecke, M. (1987). Aerodynamic and mechanical-properties of the antennae as air-current sense-organs in *Locusta migratoria*. 2. Dynamic characteristics. *J. Comp. Physiol. A* **161,** 671-680.
Heran, H. (1957). Die Bienenantenne Als Messorgan Der Flugeigengeschwindigkeit. *Naturwissenschaften* **44**, 475.
Homberg, U., Christensen, T. A. and Hildebrand, J. G. (1989). Structure and function of the deutocerebrum in insects. *Annu. Rev. Entomol.* **34**, 477-501.
Honegger, H. W., Allgäuer, C., Klepsch, U. and Welker, J. (1990). Morphology of antennal motoneurons in the brains of two crickets, *Gryllus bimaculatus* and *Gryllus campestris*. *J. Comp. Neurol.* **291**, 256-268.
Horsmann, U., Heinzel, H. G. and Wendler, G. (1983). The phasic influence of self-generated air current modulations on the locust flight motor. *J. Comp. Physiol.* **150**, 427-438.
Kennedy, J. S. and Marsh, D. (1974). Pheromone-regulated anemotaxis in flying moths. *Science* **184**, 999-1001.
Kisch, J. and Haupt, S. S. (2009). Side-specific operant conditioning of antennal movements in the honey bee. *Behav. Brain Res.* **196**, 131-133.
Kloppenburg, P. (1995). Anatomy of the antennal motoneurons in the brain of the honeybee (*Apis mellifera*). *J. Comp. Neurol.* **363**, 333-343.
Kloppenburg, P., Camazine, S. M., Sun, X. J., Randolph, P. and Hildebrand, J. G. (1997). Organization of the antennal motor system in the sphinx moth *Manduca sexta*. *Cell Tissue Res.* **287**, 425-433.
Mamiya, A., Straw, A. D., Tómasson, E. and Dickinson, M. H. (2011). Active and passive antennal movements during visually guided steering in flying *Drosophila*. *J. Neurosci.* **31**, 6900-6914.
Markl, H. (1962). Borstenfelder an Den Gelenken Als Schweresinnesorgane Bei Ameisen Und Anderen Hymenopteren. *Z. Vgl. Physiol.* **45**, 475-569.
Mielke, A. and Heide, G. (1993). Effects of artificially generated haltere nerve afferences on the activation of the flight steering muscles in *Calliphora*. In *Gene-Brain-Behaviour. Proceedings of the 21st Göttingen Neurobiology Conference* (ed. N. Elsner and M. Heisenberg), p. 207. Stuttgart: Thieme.

Niehaus, M. (1981). Flight and flight control by the antennae in the small tortoiseshell (*Aglais urticae* L., Lepidoptera). *J. Comp. Physiol.* **145**, 257-264.
Niehaus, M. and Gewecke, M. (1978). Antennal movement apparatus in small tortoiseshell (*Aglais urticae* L, Insecta, Lepidoptera). *Zoomorphologie* **91**, 19-36.
Okada, J. and Toh, Y. (2000). The role of antennal hair plates in object-guided tactile orientation of the cockroach (*Periplaneta americana*). *J. Comp. Physiol. A* **186**, 849-857.
Okada, J. and Toh, Y. (2001). Peripheral representation of antennal orientation by the scapal hair plate of the cockroach *Periplaneta americana*. *J. Exp. Biol.* **204**, 4301-4309.
Okada, J. and Toh, Y. (2006). Active tactile sensing for localization of objects by the cockroach antenna. *J. Comp. Physiol. A* **192**, 715-726.
Pearson, K. G., Wong, R. K. S. and Fourtner, C. R. (1976). Connexions between hair-plate afferents and motoneurones in the cockroach leg. *J. Exp. Biol.* **64**, 251-266.
Rospars, J. (1988). Structure and development of the insect antennodeutocerebral system. *Int. J. Insect Morphol. Embryol.* **17**, 243-294.
Sane, S. P. and Jacobson, N. P. (2006). Induced airflow in flying insects II. Measurement of induced flow. *J. Exp. Biol.* **209**, 43-56.
Sane, S. P., Dieudonné, A., Willis, M. A. and Daniel, T. L. (2007). Antennal mechanosensors mediate flight control in moths. *Science* **315**, 863-866.
Sane, S. P., Srygley, R. B. and Dudley, R. (2010). Antennal regulation of migratory flight in the neotropical moth *Urania fulgens*. *Biol. Lett.* **6**, 406-409.
Scheiner, R., Schnitt, S. and Erber, J. (2005). The functions of antennal mechanoreceptors and antennal joints in tactile discrimination of the honeybee (*Apis mellifera* L.). *J. Comp. Physiol. A* **191**, 857-864.
Schneider, D. (1964). Insect antennae. *Annu. Rev. Entomol.* **9**, 103-122.
Trimarchi, J. R., Jin, P. and Murphey, R. K. (1999). Neuromuscular junctions in *Drosophila*. In *International Review of Neurobiology*, Vol. 43 (ed. V. Budnick and L. S. Gramates), pp. 241-264. San Diego, CA: Academic Press.
Tripathy, S. J., Peters, O. J., Staudacher, E. M., Kalwar, F. R., Hatfield, M. N. and Daly, K. C. (2010). Odors pulsed at wing beat frequencies are tracked by primary olfactory networks and enhance odor detection. *Front Cell. Neurosci.* **4**, 1.
Verspui, R. and Gray, J. R. (2009). Visual stimuli induced by self-motion and object-motion modify odour-guided flight of male moths (*Manduca sexta* L.). *J. Exp. Biol.* **212**, 3272-3282.
Vickers, N. J. (2000). Mechanisms of animal navigation in odor plumes. *Biol. Bull.* **198**, 203-212.
Willis, M. A. and Arbas, E. A. (1991). Odor-modulated upwind flight of the sphinx moth, *Manduca sexta* L. *J. Comp. Physiol. A* **169,** 427-440.
Willis, M. A. and Arbas, E. A. (1998). Variability in odor-modulated flight by moths. *J. Comp. Physiol. A* **182**, 191-202.
Zar, J. H. (1999). *Biostatistical Analysis*. Upper Saddle River, NJ: Prentice-Hall.